Circularly Polarized Aperture-Coupled Microstrip Antenna for Nano-Satellites

Filipe G. Ferreira, Juner M. Vieira, Diego P. Fumagalli, Lucas S. Pereira and Marcos V. T. Heckler

***Abstract*—In this paper, the design of an aperture-coupled microstrip antenna to be installed onto a nano-satellite is described. The proposed antenna has been optimized to operate at 2.26 GHz (S-Band), which is the operating frequency of the downlink channel of the Brazilian System for Meteorological Data Acquisition. The electromagnetic analysis is done by using HFSS software. For the design validation, prototypes were manufactured and the comparison between simulations and measurements indicates good performance of the proposed antenna.**

***Keywords*—Microstrip Antenna, Aperture-Coupled Antenna, Satellite Communications.**

I. Introduction

The satellites of the Brazilian Meteorological Data Collecting System (in Portuguese, *Sistema Brasileiro de Coleta de Dados* - SBCD) are in operation over more than fifteen years, which is beyond their expected lifetime. In order to replace these satellites, the National Institute for Space Research (INPE) started the CONASAT program, which aims at providing a new and much cheaper solution for the SBCD by using a constellation of nano-satellites. The ground section of the SBCD is composed of data collecting platforms (PCDs), which have been deployed over the whole Brazilian territory including the Atlantic coast, and the Data Collection and Mission Control Center (in Portuguese, *Centro de Missão e Coleta de Dados* - CMCD) [1], [2]. Since some of the PCDs have been deployed in remote areas, such as in the Amazon region or even in the Atlantic ocean, where no internet access is available, the nano-sats will serve as data relay for retransmitting the meteorological data collected by the PCDs to the CMCD. The size of the CONASAT nano-satellite is $8U$, according to the cubesat standards developed by the Space Flight Laboratory of Toronto University. This is equivalent to a cube with 20 cm of edge size and a maximum mass of 10 kg. Since energy in space is a critical issue, the nano-sat will be equipped with four articulated flaps, so as to increase the area for installing solar panels [3].

The uplink channel for transmitting the data from the ground to the satellites works at 401 MHz (UHF) and a four-element microstrip antenna array with extended ground plane has been designed for this purpose [4]. For the downlink channel, another microstrip array will be needed, since this link operates at 2.26 GHz (S-band). In this paper, the design and the performance of an antenna for the downlink installed onto the nano-satellite is described. For this study, all electromagnetic analysis are done using commercial software and the performance is validated with measured results.

Filipe G. Ferreira, Juner M. Vieira, Diego P. Fumagalli, Lucas S. Pereira and Marcos V. T. Heckler are with Electromagnetics, Microwaves and Antennas Laboratory (LEMA), Federal University of Pampa (UNIPAMPA), Alegrete, RS, Brazil. E-mails: juner.vieira@alunos.unipampa.edu.br, lucaspereira@unipampa.edu.br, marcos.heckler@unipampa.edu.br. This work was partially supported by the Brazilian Space Agency (AEB).

For aerospace applications, the communication system is very important. In this context, the antennas play an important role. Along with other important components of a satellite, the antenna must exhibit low weight and low volume. These are characteristics intrinsic to microtrip antenna technology, which, among other advantages, present design flexibility [5]. The authors in [6] proposed an active microstrip antenna array for navigation application. In [7], an antenna array in S-band for data downlink for nano-satellite applications is presented. In [8], the integration of two antenna arrays on thin substrate simultaneously operating in S-Band and X-Band is discussed.

The antenna proposed in this paper has been designed to be compatible for installation onto a nano-satellite of the CONASAT Program. The following specifications apply for the antenna: operating frequency at 2.26 GHz, right-hand circular polarization (RHCP) with axial ratio lower than 3 dB, gain around 6 dBi, input impedance matched to 50 Ω and bandwidth of 50 MHz [3].

The paper is organized in the following sections: in section II, the details regarding the design of the single element with two linear orthogonal polarizations is discussed; sections III and IV present the design and construction of the prototypes; the final remarks are presented in section V.

II. Structure of the Single Element

Energy is an important issue when designing a satellite. For this reason, optimum antenna operation is required. For the proposed design, the microstrip antenna is fed by employing aperture coupling. By doing so, the feeding lines can be easily implemented in stripline technology, hence the pattern is not disturbed by spurious radiation. Moreover, the use of this technique results in circular polarization with high purity [9], [10].

The proposed single element is composed of three dielectric layers. Figure 1 shows the cross-sectional view of the designed structure. The material used for the top and bottom layers is R04003C with $\varepsilon_r = 3.49$ and thickness of 1.524 mm. The intermediate laminate is RO4360G2 with $\varepsilon_r = 6.15$ and thickness of 0.610 mm. The prepeg Fast Rise 27 (FR27) was used to glue the three layers. The electrical characteristics of FR27 are: dielectric constant $\varepsilon_r = 2.75$ and thickness of 0.105 mm.

In a standard aperture-coupled microstrip antenna, the patch length, feed line width and slot length are the physical pa-

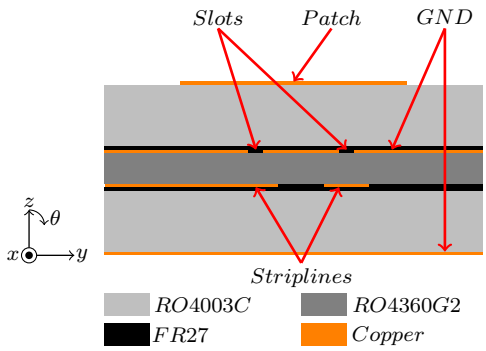

Fig. 1. Cross-sectional view of the designed antenna.

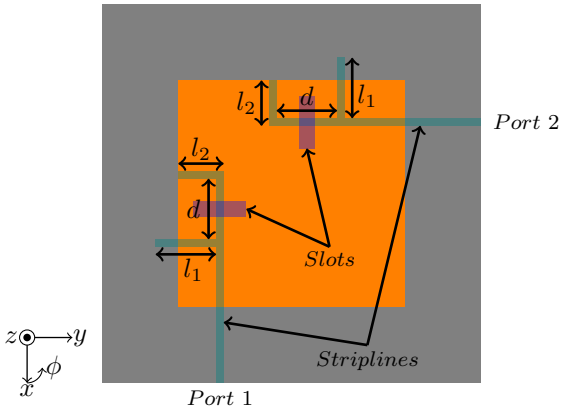

Fig. 2. Schematic top view of the designed antenna.

rameters for optimization in terms of frequency of operation and impedance matching [5]. In the proposed design, a square patch is used due to the need of circular polarization. The coupling level is determined by the slot length: the larger the slot, the stronger the coupling between the patch and the feed line. However, increasing the slot length results in power loss by excitation of surface waves [6], [11]. Therefore, the slots used in this design are small (non-resonating) and the impedance matching is ensured by employing the double-stub technique [12]. The patch length is chosen so as to tune the antenna to the maximum possible gain in the operating frequency. Once the lengths for patch and slots have been defined, impedance matching is achieved only by varying the lengths of both stubs.

Circular polarization can be obtained exciting two orthogonal modes (TM_{10}^z and TM_{01}^z) in the patch. These two orthogonal modes are excited by using two slots and by introducing a $\pm 90°$ phase shift between them, whereby the $\pm$ sign governs whether the sense of rotation of the electric field is to the right (right-hand circular polarization) or to the left (left-hand circular polarization).

III. Preliminary Antenna Design

The antenna design procedure started with the impedance matching for the antenna with two feeding lines. Since circular polarization is required, Ports 1 and 2 were fed with signals presenting $90°$ phase shift between them. This generates a radiation pattern with RHCP as principal polarization. The geometry of the element is shown in Figure 2. As commented before, impedance matching is done mostly by adjusting the lengths of the stubs. The distance between the slots and the patch center governs the coupling between the two feeding lines and has direct influence on the axial ratio (AR): the larger the coupling, the poorer the axial ratio. After the optimization process, the physical dimensions obtained are presented in Table I.

The variation of impedance as a function of frequency in the Smith Chart can be observed in Figure 3. The simulated AR as a function of the frequency and as a function of the elevation angle (θ) is shown in Figures 4 and 5, respectively. At 2.26 GHz, the axial ratio is below 1.2 dB in the boresight direction. By considering values of AR below 3 dB, the field of view with acceptable AR is $130°$ at the center operation frequency.

TABLE I
Dimensions of the Designed Antenna.

Parameter	Dimension (in mm)
Substrate size	80.80
Patch size	34.64
Distance between stubs (d)	10.66
Length stub 1 (l_1)	11.20
Length stub 2 (l_2)	6.60
Length slot	9.00
Width slot	1.80
Slot displacement from the center of the patch	9.40
Width feeding stripline	0.66

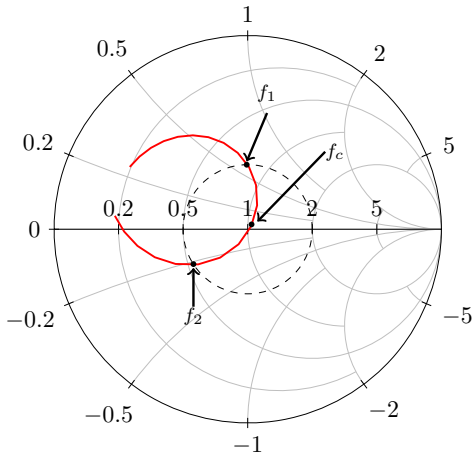

Fig. 3. Input impedance as a function of frequency in the impedance Smith chart.

In order to validate the design, a prototype was manufactured and a photo of it is presented in Figure 6. The comparison between simulated and measured S-parameters is shown in Figure 7. The parameters S_{12} and S_{21} were the same in both simulated and measured results; hence only S_{21} is plotted. High isolation between the ports was obtained. Frequency shift of 14 MHz for the S_{11} parameter and 21 MHz for S_{22} were verified.

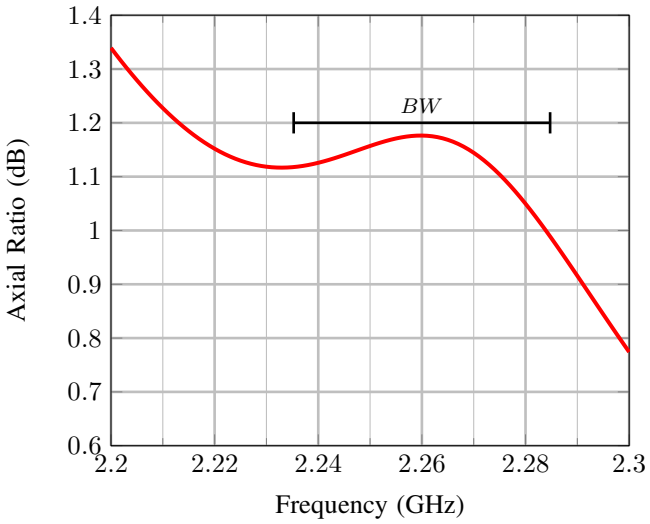

Fig. 4. Simulated axial ratio as a function of the frequency for the designed antenna.

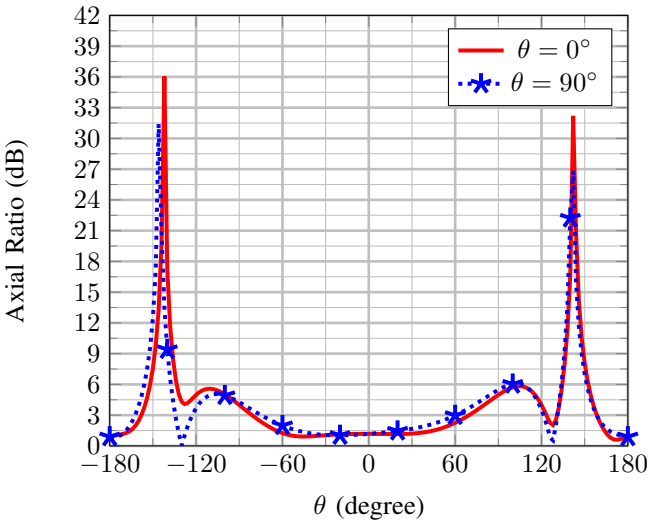

Fig. 5. Simulated axial ratio as a function of the elevation angle for the designed antenna.

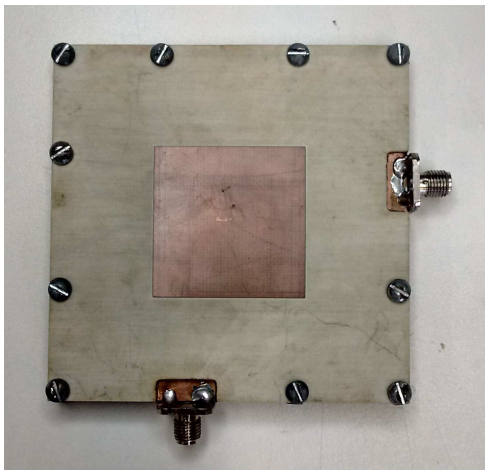

Fig. 6. Top view of the prototype.

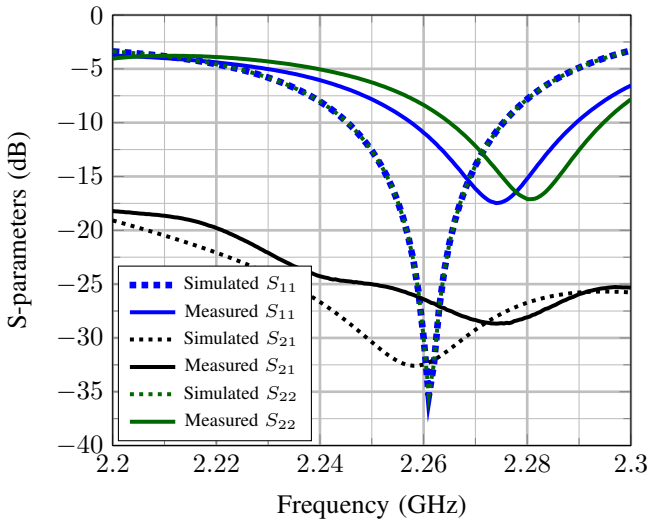

Fig. 7. Comparison between simulated and measured S-parameters for the designed antenna.

To investigate this discrepancies, a parametric study of the dielectric constant of the laminate RO4003C was done by keeping the original antenna dimensions. In this new simulation, the use of $\varepsilon_r = 3.43$ instead of 3.49 for the RO4003C laminate resulted in good agreement with the measured curves. The comparison between simulation results using $\varepsilon_r = 3.43$ and the experimental data is shown in Figure 8.

The radiation pattern measurements have been carried out using a spherical near-field scanner (NFS), which calculates the far fields from the sampled near field. For introducing a 90° phase shift between the input ports, an external 90°-hybrid was connected to the antenna inputs. A photo showing the measurement setup is presented in Figure 9. Figure 10 presents the comparison between simulated and measured normalized radiation patterns. The simulated maximum gain obtained for this antenna is 6.01 dBi and the Half-Power Beamwidth (HPBW) obtained is 84°. One can observe that very good agreement for the principal polarization was obtained, and high cross-polarization decoupling in the boresight, more than 25 dB, is verified.

IV. Antenna with an Integrated 90° Hybrid Coupler

The proposed antenna has two feeding points for exciting two orthogonal modes. Also, a 90° phase shift between the signals is necessary so that circularly polarized (CP) waves can be transmitted. So, a design of the of 90° hybrid was realized in stripline technology. After optimizations for the 90° phase difference at the outputs at the operation frequency, the physical dimensions of the hybrid are listed in Table II according to the convention sketched in Figure 11.

Thus, using the dimensions given in Tables I and II, simulations with an integrated 90° hybrid were done. In this case, the dielectric constant of the laminate RO4003C used was $\varepsilon_r = 3.43$. The resulting geometry can be seen in Figure 11.

The simulated S-parameters with the frequency are presented in Figure 12. The simulated AR as a function of

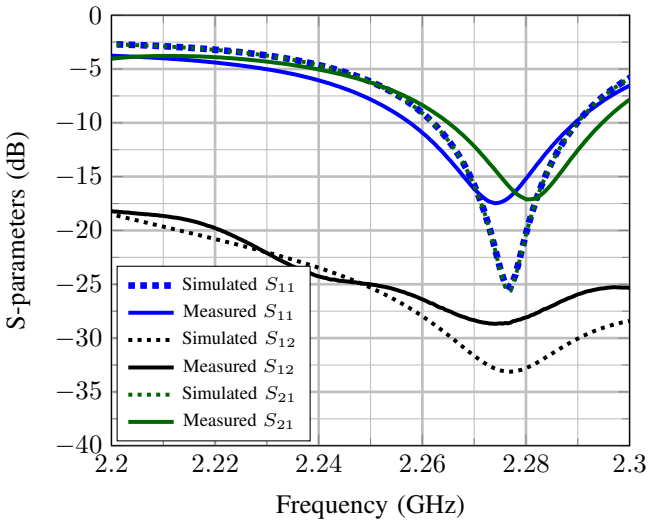

Fig. 8. Comparison between simulated (using $\varepsilon_r = 3.43$) and measured S-parameters for the designed antenna.

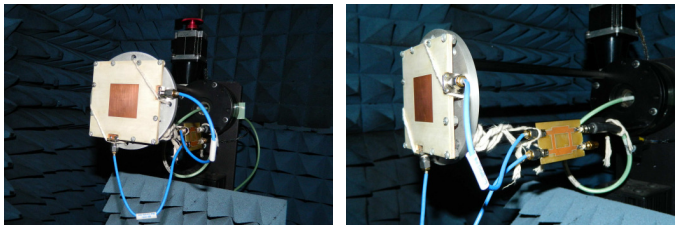

(a) (b)

Fig. 9. Prototype with an external 90° Hhybrid mounted in spherical near-field scanner.

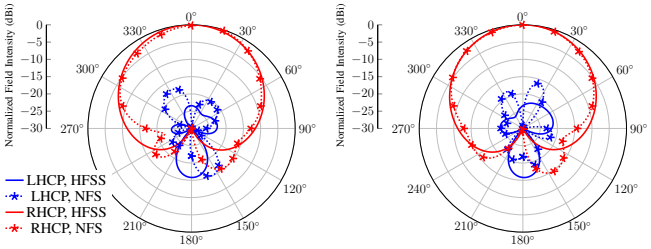

(a) Plane $\phi = 0°$. (b) Plane $\phi = 90°$.

Fig. 10. Comparison between simulated and measured radiation patterns.

TABLE II
DIMENSIONS OF THE 90° HYBRID.

Parameter	Dimension (in mm)
$L_{50\Omega}$	14.62
$W_{50\Omega}$	0.66
$L_{35.35\Omega}$	14.54
$W_{35.35\Omega}$	1.30

the frequency and of the elevation angle (θ) are shown in Figures 13 and 14, respectively. It is observed that the AR is below 3 dB for an angular region of approximately 130°. The simulated gain pattern was plotted and is shown in Figure 15. Large cross-polarization decoupling can be observed. The

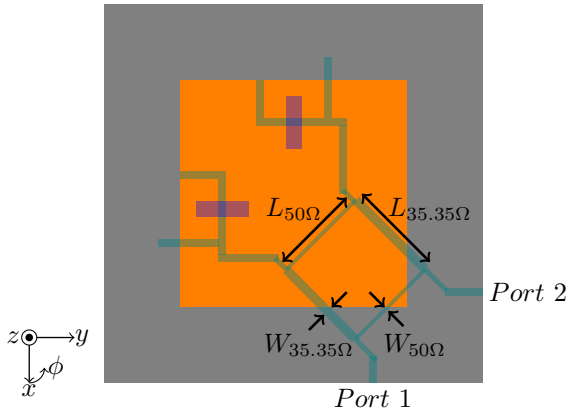

Fig. 11. Schematic top view of the designed antenna with an integrated 90° Hybrid.

maximum gain obtained for this antenna was 5.97 dBi.

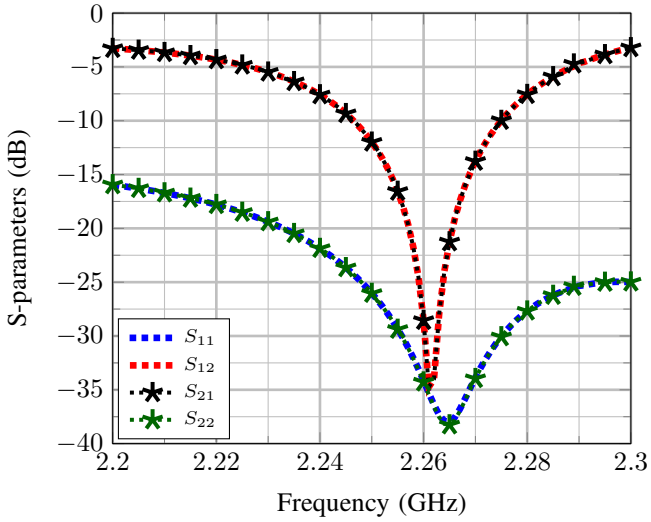

Fig. 12. Variation of the S-parameters with the frequency for the antenna with an integrated 90° Hybrid.

V. CONCLUSIONS

In this paper, the design of an RHCP microstrip antenna operating in the S-band for nano-satellite has been described. The design started with impedance matching between the patch and two feeding lines. This model exhibits two orthogonal linear polarizations and was manufactured and measured. The simulated gain of the antenna operating at 2.26 GHz was 6.01 dBi. Although the measured S-parameters presented a frequency deviation, which has been attributed to the dielectric constant value used in the simulations, the measured gain pattern showed good agreement with the simulations and large cross-polarization decoupling was obtained. The second design step was to develop and to integrate a 90° hybrid into the antenna structure. In terms of axial ratio and gain, the results obtained were similar to the linearly polarized geometry with an external 90° hybrid. The next steps of this work are the construction of a prototype with an integrated hybrid and the

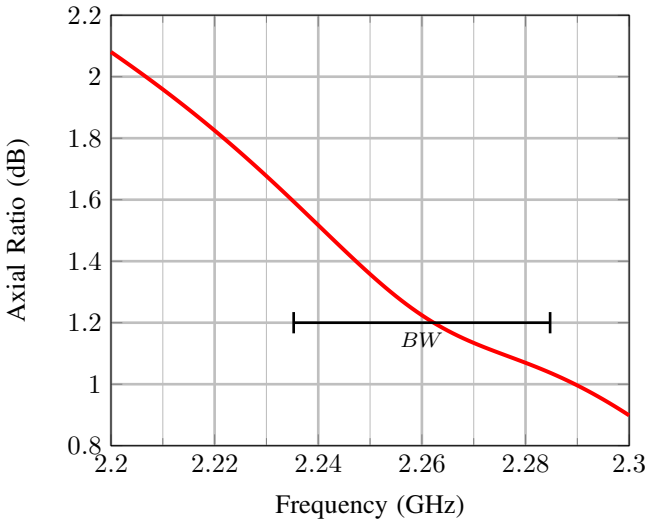

Fig. 13. Simulated axial ratio as a function of the frequency for the antenna with an integrated 90° Hybrid.

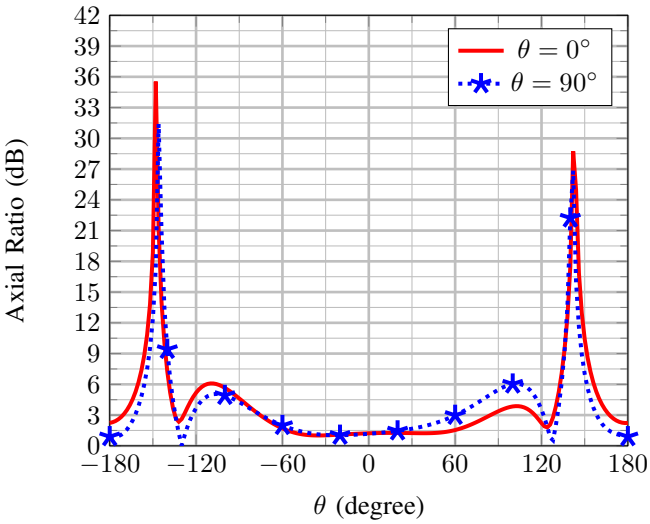

Fig. 14. Simulated axial ratio as a function of the elevation angle for the antenna with an integrated 90° Hybrid.

study of the feasibility to compose an array with the proposed antenna.

ACKNOWLEDGEMENTS

This work has been partially supported by Brazilian Space Agency (AEB) under the frame of the UNIESPAÇO Program.

REFERENCES

[1] M. J. M. de Carvalho, J. S. dos Santos Lima, L. dos Santos Jotha, and P. S. de Aquino, "CONASAT - Constelação de Nano Satélites para Coleta de Dados Ambientais," *XVI Simpósio Brasileiro de Sensoriamento Remoto*, pp. 9108–9115, 2013.

[2] W. Yamaguti, V. Orlando, and S. Pereira, "Sistema Brasileiro de Coleta de Dados Ambientais: Status e Planos Futuros," *XIV Simpósio Brasileiro de Sensoriamento Remoto*, vol. 14, pp. 1633–1640, 2009.

[3] J. S. dos Santos Lima, L. dos Santos Jotha, and R. B. Biondi, *Documento de Descrição da Missão (DDM)*, Centro Regional do Nordeste - Instituto Nacional de Pesquisas Espaciais (CRN/INPE), Natal-RN, 2011. [Online]. Available: http://www.crn2.inpe.br/conasat1/docprojeto.php

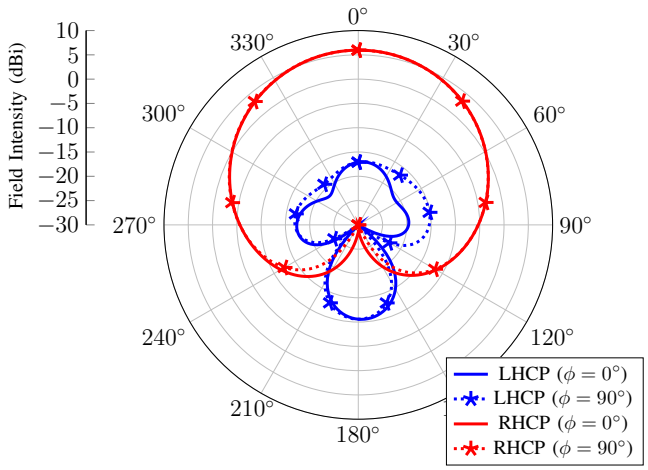

Fig. 15. Simulated gain pattern for different elevation planes.

[4] J. M. Vieira, M. P. Magalhães, M. V. T. Heckler, J. C. M. Mota, and A. S. Sombra, "Development of an UHF 2 x 2 Microstrip Antenna Array for Nano-Satellites," *Journal of Communication and Information Systems*, vol. 31, no. 1, 2016, DOI:10.14209/jcis.2016.13.

[5] C. A. Balanis, *Antenna Theory: Analysis and Design*. John Wiley & Sons, 2005, vol. 1.

[6] M. V. T. Heckler, W. Elmarissi, L. A. Greda, M. Cuntz, and A. Dreher, "Narrow-Band Microstrip Antenna Array for a Robust Receiver for Navigation Applications," in *Antennas and Propagation, 2009. EuCAP 2009. 3rd European Conference on*. IEEE, 2009, pp. 1206–1210.

[7] T. Sreeja, A. Arun, and J. Jaya Kumari, "An S-Band Micro-strip Patch Array Antenna for Nano-Satellite Applications," in *Green Technologies (ICGT), 2012 International Conference on*. IEEE, 2012, pp. 325–328, DOI:10.1109/ICGT.2012.6477994.

[8] S. H. Hsu, Y. J. Ren, and K. Chang, "A Dual-Polarized Planar-Array Antenna for S-Band and X-Band Airborne Applications," *Antennas and Propagation Magazine, IEEE*, vol. 51, no. 4, pp. 70–78, 2009, DOI:10.1109/MAP.2009.5338685.

[9] D. M. Pozar, "Microstrip Antenna Aperture-Coupled to a Microstripline," *Electronics Letters*, vol. 21, no. 2, pp. 49–50, January 1985, DOI:10.1049/el:19850034.

[10] K. M. Luk, T. M. Au, K. F. Tong, and K. F. LEE, *Aperture-Coupled Multilayer Microstrip Antennas*. John Wiley & Sons, ch. 2, pp. 71 – 122.

[11] M. P. David, "A Review of Aperture Coupled Microstrip Antennas: History, Operation, Development, and Applications by," 1996.

[12] D. M. Pozar, *Microwave Engineering*. John Wiley & Sons, 2009.